Int. J. Heat Mass Transfer. Vol. 28, No. 3, pp. 603–612, 1985
Printed in Great Britain

0017–9310/85 $3.00 + 0.00

A numerical study of two-dimensional laminar natural convection in shallow open cavities

Y. L. CHAN
Department of Aerospace and Mechanical Engineering, University of Notre Dame, Notre Dame, IN 46556, U.S.A.

and

C. L. TIEN
Department of Mechanical Engineering, University of California, Berkeley, CA 94720, U.S.A.

(*Received* 27 *February* 1984 *and in final form* 4 *September* 1984)

Abstract—Laminar steady-state natural convection in a two-dimensional rectangular open cavity is investigated numerically. Isotherms and streamline plots are obtained in a shallow open cavity with aspect ratio of 0.143 for Rayleigh numbers up to 10^6 using constant properties and Boussinesq approximations, by imposing approximate boundary conditions at the opening. This method has been tested and compared to cases where computations are carried out into an enlarged external domain. Results show that outgoing flow patterns and the heat transfer results are governed by strong characteristics of the heated cavity. These findings compare favorably with experimental results for $Ra = 10^6$.

INTRODUCTION

NATURAL convection in enclosures has received a lot of attention [1, 2] because of interests in building insulation, passive solar heating and many environmental geothermal flow processes. A related problem for an open cavity or partial enclosure geometry has not been investigated as extensively. Some recent numerical and experimental studies on open cavities have been performed in modeling solar thermal central receiver systems [3, 4, 5, 6, 7], fire spread in rooms [8], circulation above city streets and geothermal reservoirs [9, 10]. These papers all involved rectangular geometries with aspect ratio close to unity.

Natural convection in shallow horizontal open cavities (with a small height-to-length aspect ratio) occurs in engineering systems where there is a temperature difference between the cavity wall and the fluid reservoir with which the cavity is connected. Such flows can be found in pipes joining fluid reservoirs at different temperatures; these include cryogenic fluid storage and nuclear reactor transfer systems. Other examples involve applications in heat transfer augmentation. Chan and Tien [11] investigated flows in a two-dimensional shallow open cavity using laser Doppler velocimetry. The purpose of this paper is to study the problem numerically and to make a comparison with experimental results.

PROBLEM FORMULATION

The geometry of the two-dimensional cavity is illustrated in Fig. 1. It has one heated vertical wall at temperature T_H and an opening to the ambient or a fluid reservoir which is at a characteristic temperature T_∞. The top and bottom horizontal walls are insulated.

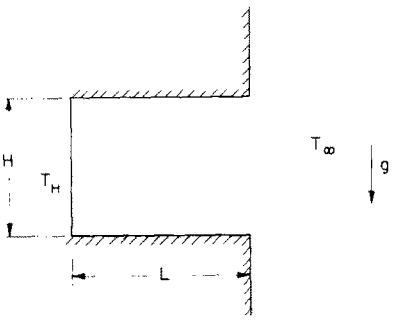

FIG. 1. Open cavity geometry.

The continuity, momentum and energy equations governing a two-dimensional laminar flow of a Newtonian fluid, with no dissipation, can be written as the following, with gravity acting in the vertical $-y$ direction

$$\frac{\partial \rho}{\partial t} + \frac{\partial}{\partial x}(\rho u) + \frac{\partial}{\partial y}(\rho v) = 0 \tag{1}$$

$$\frac{\partial}{\partial t}(\rho u) + \frac{\partial}{\partial x}(\rho u^2) + \frac{\partial}{\partial y}(\rho uv) = -\frac{\partial p}{\partial x} + \frac{\partial}{\partial x}\left(\mu \frac{\partial u}{\partial x}\right) + \frac{\partial}{\partial y}\left(\mu \frac{\partial u}{\partial y}\right) \tag{2}$$

$$\frac{\partial}{\partial t}(\rho v) + \frac{\partial}{\partial x}(\rho uv) + \frac{\partial}{\partial y}(\rho v^2) = -\frac{\partial p}{\partial y} - \rho g + \frac{\partial}{\partial x}\left(\mu \frac{\partial v}{\partial x}\right) + \frac{\partial}{\partial y}\left(\mu \frac{\partial v}{\partial y}\right) \tag{3}$$

NOMENCLATURE

B	ratio of length to height, L/H
c_p	specific heat at constant pressure
g	gravitational acceleration, in $-y$ direction
Gr	Grashof number, $g\beta\Delta TH^3/\nu^2$
H	height of cavity
k	thermal conductivity of fluid
L	length of cavity
$\dot{M}$	dimensionless volumetric flow rate through opening in cavity, equation (14)
Nu	Nusselt number, equation (13)
P	dimensionless pressure
p	pressure
p_∞	ambient pressure
Pr	Prandtl number, ν/α
Ra	Rayleigh number
T	dimensionless temperature
T°	temperature
T_f	film temperature, $(T_H + T_\infty)/2$
T_H	hot wall temperature
T_∞	ambient temperature
ΔT	temperature difference, $T_H - T_\infty$
t	time
U	dimensionless velocities in x-direction
u	velocities in x-direction
V	dimensionless velocities in y direction
v	velocities in y-direction
X, Y	dimensionless Cartesian coordinates
X_0	X coordinate of vertical walls
x, y	Cartesian coordinate.

Greek symbols

α	thermal diffusivity
β	coefficient of volumetric thermal expansion
μ	dynamic viscosity
ν	kinematic viscosity
ρ	density of fluid
ρ_∞	fluid density at ambient
τ	dimensionless time
ψ	stream function.

Subscripts

in	into cavity
∞	ambient values
out	out of cavity.

$$\frac{\partial}{\partial t}(\rho c_p T^\circ) + \frac{\partial}{\partial x}(\rho u c_p T^\circ) + \frac{\partial}{\partial y}(\rho v c_p T^\circ) = \frac{\partial}{\partial x}\left(k\frac{\partial T^\circ}{\partial x}\right) + \frac{\partial}{\partial y}\left(k\frac{\partial T^\circ}{\partial y}\right). \quad (4)$$

It is convenient to subtract from the momentum equations, the static equilibrium equations:

$$\frac{\partial p_\infty}{\partial x} = 0; \quad \frac{\partial p_\infty}{\partial y} = -\rho_\infty g. \quad (5)$$

Assumption of constant fluid properties and the Boussinesq approximation (fluid density variations neglected except in the buoyancy term) are made. Nondimensionalized variables can be form as

$$X = \frac{x}{H}; \quad Y = \frac{y}{H}; \quad U = u\frac{H}{\alpha}; \quad V = v\frac{H}{\alpha};$$

$$\tau = \frac{\alpha}{H^2}t; \quad T = \frac{T^\circ - T_\infty}{T_H - T_\infty}; \quad P = (p - p_\infty)H^2/\rho\alpha^2. \quad (6)$$

The relevant parameters are

$$Pr = \nu/\alpha = \mu c_p/k; \quad B = L/H;$$

$$Gr = \frac{g\beta H^3(T_H - T_\infty)}{\nu^2};$$

$$Ra = Gr\,Pr = \frac{g\beta H^3(T_H - T_\infty)}{\nu\alpha} \quad (7)$$

$$\beta = -\frac{1}{\rho}\left(\frac{\rho - \rho_\infty}{T^\circ - T_\infty}\right). \quad (8)$$

The nondimensional governing equations in transient form are then

$$\frac{\partial U}{\partial X} + \frac{\partial V}{\partial Y} = 0 \quad (9)$$

$$\frac{\partial U}{\partial \tau} + \frac{\partial (U^2)}{\partial X} + \frac{\partial (UV)}{\partial Y} = -\frac{\partial P}{\partial X} + Pr\left(\frac{\partial^2 U}{\partial X^2} + \frac{\partial^2 U}{\partial Y^2}\right) \quad (10)$$

$$\frac{\partial V}{\partial \tau} + \frac{\partial (UV)}{\partial V} + \frac{\partial (V^2)}{\partial Y} = -\frac{\partial P}{\partial Y} + Ra\,Pr\,T + Pr\left(\frac{\partial^2 V}{\partial X^2} + \frac{\partial^2 V}{\partial Y^2}\right) \quad (11)$$

$$\frac{\partial T}{\partial \tau} + \frac{\partial (UT)}{\partial X} + \frac{\partial (VT)}{\partial Y} = \frac{\partial^2 T}{\partial X^2} + \frac{\partial^2 T}{\partial Y^2}. \quad (12)$$

The Nusselt number Nu is then a function of Ra, Pr, and B, and is defined here as the overall heat transfer from the heated wall to the fluid:

$$Nu \equiv \int_{\text{Wall}} -\left(\frac{\partial T}{\partial X}\right)_{X=0} dY = Nu(Ra, Pr, B). \quad (13)$$

NUMERICAL APPROACH

Many studies of natural convection in two-dimensional enclosures made use of the stream function

and vorticity as variables in their computations. However, at an open boundary, the stream function and vorticity cannot be specified. One approach to the open cavity problem has been the employment of an extended computational domain outside the opening. Penot [3] and LeQuere *et al.* [4] investigated the two-dimensional isothermal square open cavity using such approach. Chan and Tien [7] examined natural convection in a square open cavity with insulated horizontal walls as shown in Fig. 1. The boundary conditions and the computational domain used are shown in Fig. 2. There are two blocked regions (insulated solid) above and below the cavity. Primitive variables are used in developing the computer code to solve the two-dimensional steady laminar flow problem. It is based on the SIMPLER (Semi-Implicit Method for Pressure Linked Equations Revised) algorithm formulated by Patankar [12]. The same computer code is used in the present study. Descriptions of the code can be found in [7, 13]. Previous studies [4, 7] have shown that the solutions in the cavity and the near-field are insensitive to the ways the approximate boundary conditions are set, as long as the outer boundaries are sufficiently far from the opening. The heated cavity, therefore, exhibits a strong characteristic of its own. The flow and heat transfer in the cavity and a region just local to the opening (marked by an internal rectangle in Fig. 2) can then be taken as the correct results.

In the case of a shallow open cavity, there is motivation to try a simpler approach of restricting the computation to within the cavity. From cost and feasibility consideration, exclusion of the extended

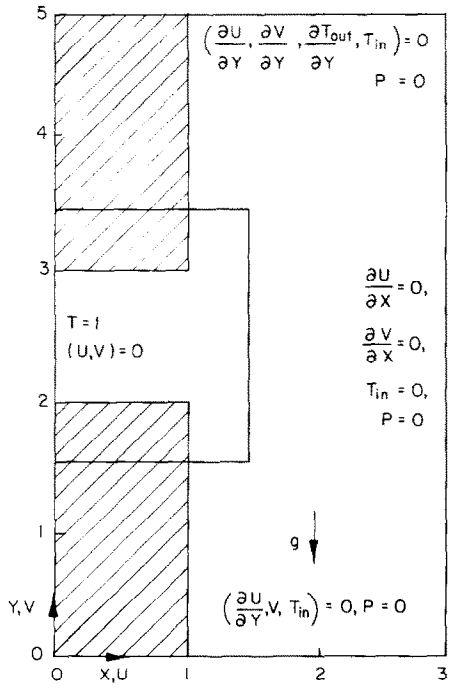

FIG. 2. Boundary conditions for Method A.

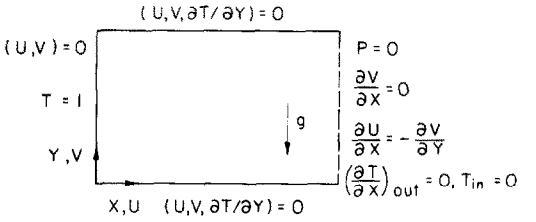

FIG. 3. Boundary conditions for Method B.

outer region and the blocked region will save memory space and computational time. Figure 3 shows the computational domain and boundary conditions used in a simplified approach, hereby called Method B, for a rectangular open cavity. This should be distinguished from Method A which refers to the one with an extended computational domain. The geometry in Method B has a solid heated wall on the left. The top and bottom horizontal walls are insulated. At the opening, temperatures of fluid coming from the ambient region are set to zero and temperatures of fluid going out satisfy the upwind condition, assuming convection to be predominant. The velocity gradient for V, the vertical velocity, is set at zero. The boundary condition for U, the horizontal velocity, is obtained by the mass balance at the boundary cells, that is, $\partial U/\partial X = -\partial V/\partial Y$.

Before applying the simplified approach, Method B, to the shallow open cavity computations, this approach is tested in a square open cavity geometry. Results from using Method A [7], with an extended domain, serve as a standard for comparison. It will be shown that the simplified approach gives good heat transfer results and the basic flow patterns inside the cavity. Its shortcoming will also be discussed in the following section.

COMPARISON OF RESULTS FOR SQUARE CAVITY

Method A with an extended computational domain uses a 41 × 52 variable grid system. Method B has 31 × 30 grid points. Table 1 shows a comparison of Nu and $\dot{M}$, the volumetric flow rate through the cavity, for the two methods for $Pr = 1$, $B = 1$ (square), $Ra = 10^3, 10^6$ and 10^9. Definitions of $\dot{M}$ and stream function ψ are

$$\dot{M} = -\int_{\substack{\text{Opening} \\ X=1}} U_{in}\,dY \quad \text{where} \quad U_{in} = U_{X=1}$$

$$\text{if} \quad U_{X=1} < 0 \tag{14}$$

Table 1. Comparisons of results from Method A (with outer region) and Method B, $Pr = 1$, $B = 1$

Ra	Nu(B)	Nu(A)	$\dot{M}$(B)	$\dot{M}$(A)
10^3	1.33	1.07	2.65	1.95
10^6	15.0	15.0	47.4	47.3
10^9	101	105	388	377

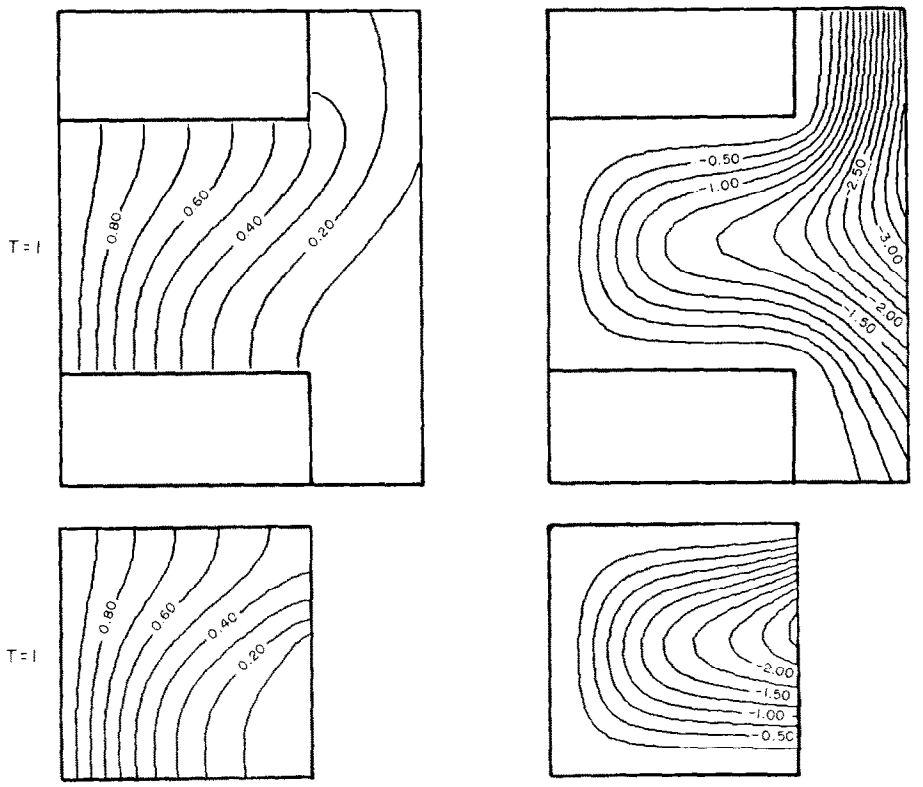

FIG. 4. Comparison of Methods A and B at $Ra = 10^3$, $Pr = 1$, $B = 1$.

or $\quad U_{in} = 0 \quad \text{if} \quad U_{X=1} > 0$

$$\psi(X, Y) = -\int_{X_0}^{X} V(X, Y)\,dX + \psi(X_0, Y). \quad (15)$$

Stream function values, $\psi(X_0, Y)$, are zero along a vertical solid boundary. Figures 4–6 compare the isotherms and streamline patterns for the two methods at different Ra.

At low Ra of 10^3, the heat transfer result from Method B is higher. This can be explained by the effect of setting $T_{in} = 0$ at the opening in the simplified approach. It compresses the isotherms and thus increases the temperature gradient and heat transfer in this conduction-dominant regime. Figure 4 illustrates this effect on the isotherm patterns. However, the flow patterns are similar.

Figure 5 shows that the isotherm patterns are essentially identical for the two methods at $Ra = 10^6$. This explains the equal values of Nu in Table 1. This is expected at moderate to high Ra where the heat transfer occurs within the boundary layer. The two values of $\dot{M}$ are equal and the flow patterns are nearly identical. Slight deviations occur at the entrance where the inflow enters at an angle when it turns around the lower corner. Without taking into account this corner, the simplified approach cannot predict such phenomenon.

At the high Ra of 10^9, as shown in Fig. 6, the corner effect becomes very significant resulting in the development of a recirculating zone. The flow patterns from the two methods differ in this aspect. However, if attention is paid mainly to the exiting flow, the strongly stratified hot fluid comes out in a similar pattern in both solutions. The isotherm patterns remain identical too due to the boundary-layer-type heat transfer and flows. The variation of the cold fluid flow pattern inside the cavity creates little differences in heat transfer. Since the same amount of heat must be carried out of the cavity by the hot fluid, the exit flow, being downstream, is determined by the condition at the heated wall.

Based on the comparisons, several observations can be made. The simplified approach can yield good heat transfer results without calculation in the extended domain. This is particularly true at higher Ra when convection becomes dominant. The heat transfer and the outgoing flow pattern is governed by a strong characteristic of the heated cavity. However, since no consideration is taken into account of the corner and outer region, the simplified approach fails to predict some of the flow characteristics like the turn and separation around the corner at high Ra. When applied to the shallow cavity case, the heat transfer rate and flow patterns are expected to be affected even less by the manner the open boundary conditions are set, because of the far distance between the two end boundaries.

SHALLOW OPEN CAVITY

Computations have been performed under the conditions of constant properties and Boussinesq

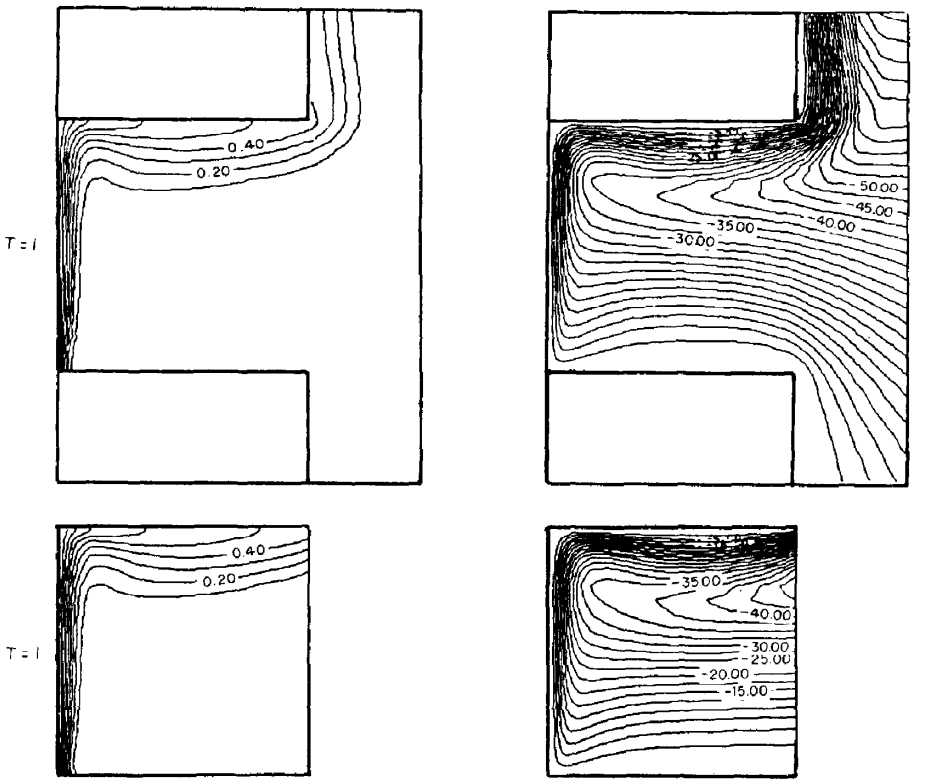

FIG. 5. Comparison of Methods A and B at $Ra = 10^6$, $Pr = 1$, $B = 1$.

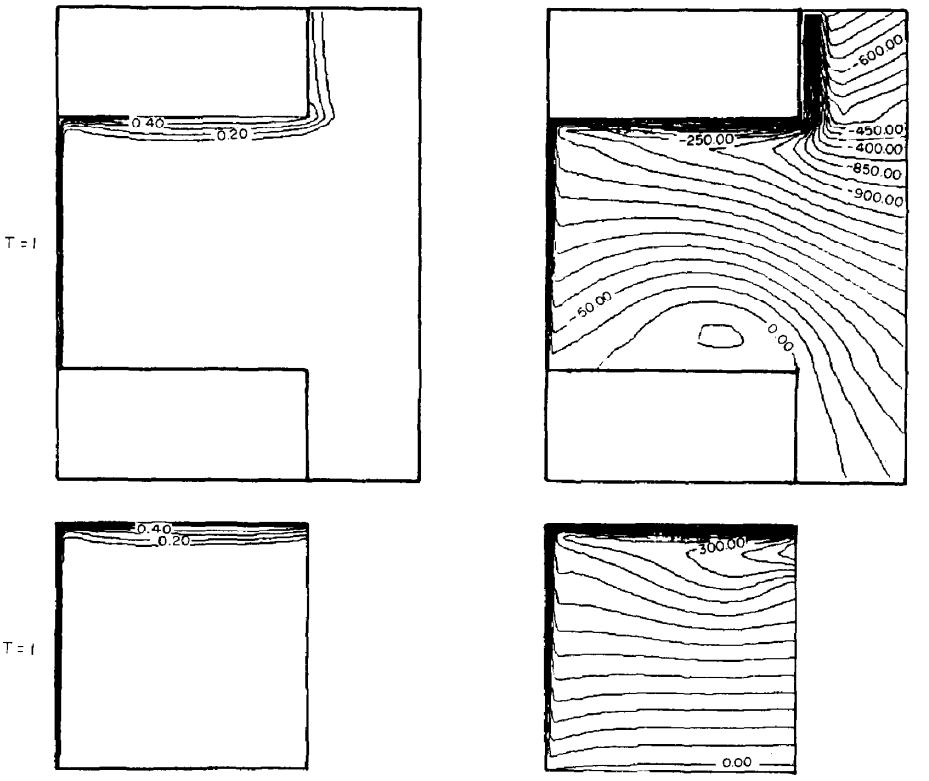

FIG. 6. Comparison of Methods A and B at $Ra = 10^9$, $Pr = 1$, $B = 1$.

approximation. Prandtl number is set at 7.0 (models water at 72°F) for a shallow cavity of aspect ratio 0.143 ($B = 7$). A 96 x 22 variable grid system is used with the boundary conditions set according to Method B, where computations are restricted to within the cavity only. The steady laminar flow condition is assumed. Heat transfer results, isotherms and flow patterns have been obtained for Ra ranging from 10^3 to 10^6.

Table 2 presents the results of the Nu vs Ra. Figures 7–10 show the isotherms and streamlines at different Ra. The vertical heated wall is on the left and the opening is on the right. The isotherms are shown on the top figures.

At the low Ra of 10^3, the heat transfer mechanism is conduction dominant. Figure 7 shows that the temperature field is only slightly distorted by the convective flow. The temperature gradient is nearly constant along the whole length of the cavity except very near the opening. This constant temperature gradient provides the driving force of the flow. The effect of the open boundary does not penetrate very far into the cavity, as marked by the location where the incoming flow turns around to exit. There is a core region where the velocity field is everywhere parallel to the horizontal walls. The core flow resembles the asymptotic solution obtained by Cormack *et al.* [14, 15] and Imberger [16] for a shallow cavity with differentially heated end walls. A stream of warm fluid flows in the upper half of the cavity and is gradually cooled as it moves from left to right by the counter flow beneath it. The heated wall serves to turn the flow around 180°.

As Ra increases, the effect of the open boundary penetrates further into the flow. At $Ra = 10^4$, Fig. 8 shows that convection disorts the isotherms considerably but a constant temperature gradient still exists. A core region of zero vertical velocities also exists. At $Ra = 10^5$, Fig. 9 shows that the boundary layer begins to form near the heated wall. The effect of the open boundary is more significant and the core region starts to disappear. The exiting flow accelerates toward the opening and its passage becomes narrower. The vertical velocities in the cavity are still small but no longer zero.

Table 2. Variations of Nu and $\dot{M}$ with Ra for the shallow open cavity $Pr = 7$, $B = 7$

Ra	10^3	10^4	10^5	10^6
Nu	0.147	0.616	5.30	15.25
$\dot{M}$	0.624	5.65	30.8	93.4

At high Ra of 10^6, the effect of the open boundary can be seen in Fig. 10, to approach near the heated wall. The bottom part of the cavity is occupied by cold fluid at ambient temperature until it reaches the heated wall. The cold fluid flow also bends slightly due to entrainment toward the bottom where maximum heat transfer occurs. The upper exit flow can be thought of as driven by the temperature difference between the vertical wall and the thermally stratified fluid. A core region no longer exists. The hot fluid accelerates toward the opening first gently and then rapidly as it approaches the open end. The flows and temperature profiles in the cavity are different from that for a closed enclosure case as symmetries do not exist.

The numerical results obtained for the shallow open cavity cases are expected to have the same drawback inherent in the simplified approach by restricting computations to within the cavity. In specifying conditions at the opening, the effects of outside conditions have not been accounted for. These include flow around the lower corner, the upward flow of the 'released' hot fluid escaping from under the restrictive horizontal wall and the entrainment to this hot plume from the surrounding fluid. For this reason, the flow patterns, especially near the opening, can only be approximate to the real case.

COMPARISON WITH EXPERIMENT

In order to compare the experimental data [11] quantitatively with the numerical solution, the

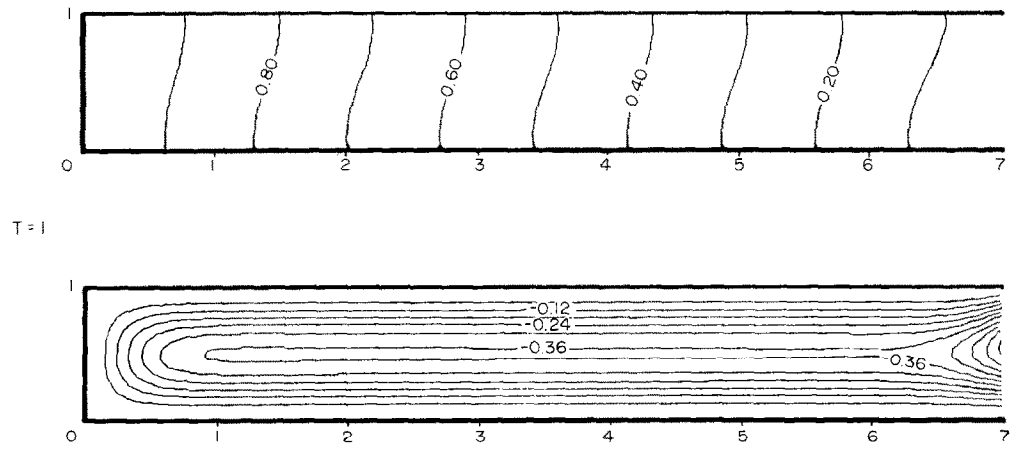

FIG. 7. Isotherms and streamlines for $Ra = 10^3$, $Pr = 7$, $B = 7$.

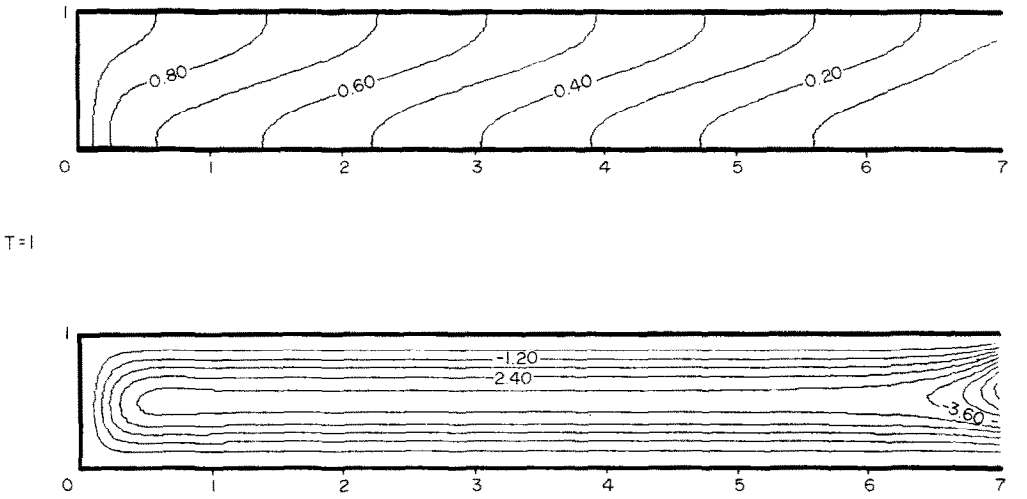

FIG. 8. Isotherms and streamlines for $Ra = 10^4$, $Pr = 7$, $B = 7$.

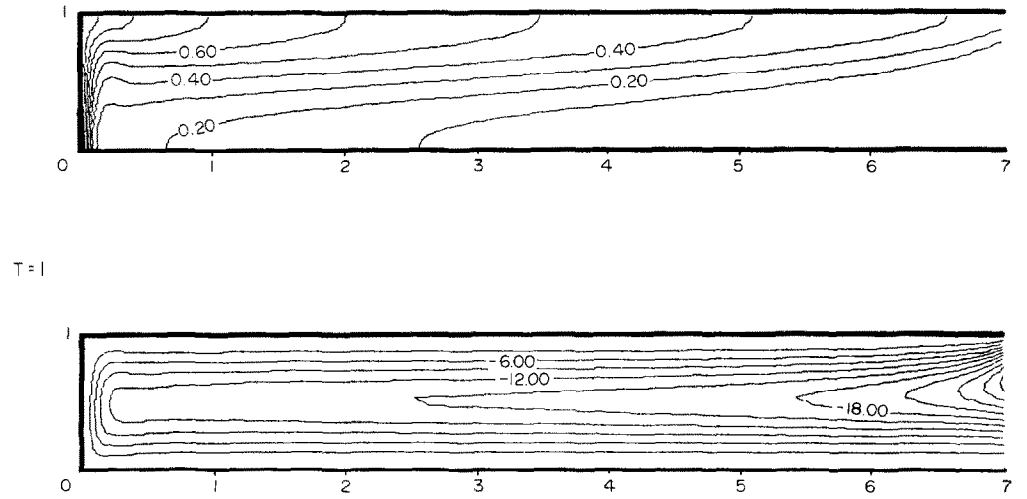

FIG. 9. Isotherms and streamlines for $Ra = 10^5$, $Pr = 7$, $B = 7$.

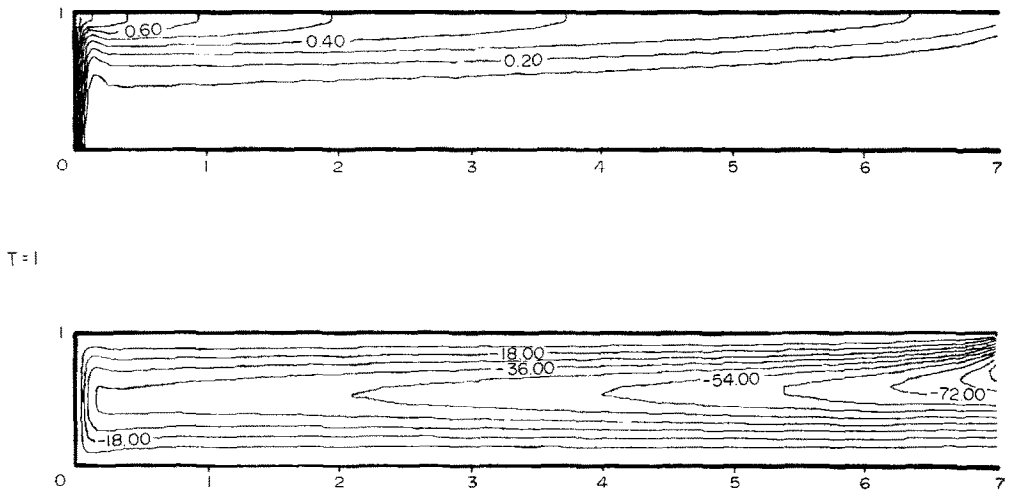

FIG. 10. Isotherms and streamlines for $Ra = 10^6$, $Pr = 7$, $B = 7$.

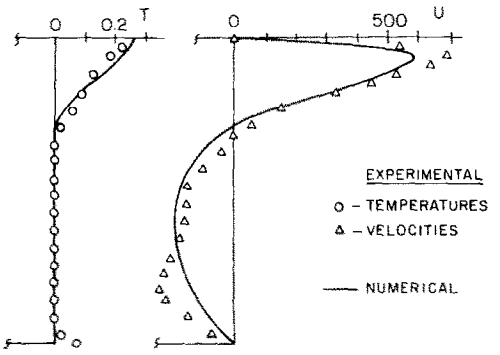

FIG. 11. Comparisons of experimental with numerical results at the opening for $Ra = 10^6$.

experimental velocities and temperatures are non-dimensionalized using equation (6). The properties are evaluated at the film temperature T_f. Figure 11 shows the nondimensionalized experimental and numerical horizontal velocities U and temperature T at the opening, for $Ra = 10^6$. The maximum of the outgoing flow is underpredicted by the numerical solution. This can be attributed to the omission of the outer region in the computations. The 'pull' by the escape of the hot buoyant fluid is not modeled in the numerical boundary conditions as $\partial V/\partial X$ has been set equal to zero. The bump in the incoming flow near the bottom is due to the unclean experimental conditions, specifically natural convection up the lower vertical wall. It has also been pointed out that the experimental data themselves involve errors of about 15% from the experimental system. The outgoing flow in the experiment occupies 31% of the opening while the numerical result gives 29%. The two temperature profiles also agree well. The temperature decreases to the ambient value at nearly the same depth. Because the measured inflow temperatures are all close to ambient, this situation precisely matches the numerical boundary condition.

Figure 12 shows the comparisons at a location $X = 4.14$, near the middle of the cavity. While the numerical solution predicts a slight difference in the outgoing and incoming flows, the experimental data

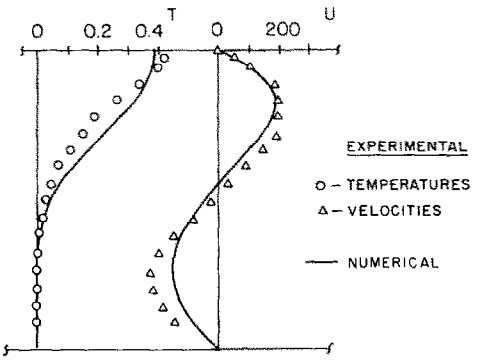

FIG. 12. Comparisons of experimental with numerical results in the cavity for $Ra = 10^6$.

give a rather symmetric flow pattern. The temperature profile for the experiment also differs slightly from the numerical solution. The overall magnitude and shape of the experimental profiles agree well with the numerical results.

The numerical solutions have not taken into account the variable properties, and other conditions specifically occurring in the experiments. They have also ignored the region outside the shallow cavity. However, from the comparisons with the experimental data, the numerical model appears to be adequate in predicting the basic flow pattern and heat transfer characteristics.

DISCUSSION

Figure 13 shows a plot of Nu vs Ra for the square cavity, shallow cavity, isothermal vertical flat plate [17] and the experimental results [11] for the shallow cavity. The length-to-height aspect ratio B is zero for the flat plate. Comparisons should be made by noting the definition of Nu in equation (13). The Nusselt number is equal to unity for a purely conduction case for a unit temperature gradient (unit temperature difference across unit length). At low Ra, Nu for the square cavity is about 1.0 and that for the shallow cavity is about 0.143, both equal to the aspect ratios. As Ra increases, both Nu for the square and the shallow cavities go through a transition where convection picks up more heat transfer. They approach the asymptotic values as heat transfer becomes predominantly determined by the boundary-layer flows up the heated wall. It can be observed that these asymptotic results are close to that for a flat plate, Nu varying with Ra to the power 0.284, independent of aspect ratio. (A value of 0.25 is usually obtained for flat plate results.) The effect of the long channel essentially delays this asymptotic behavior. A longer or shallower cavity is expected to take a higher value of Ra to reach the flat plate results. However, Ra cannot increase indefinitely without the laminar steady flow assumption breaking down near the heated wall.

Both the experimental and the numerical results

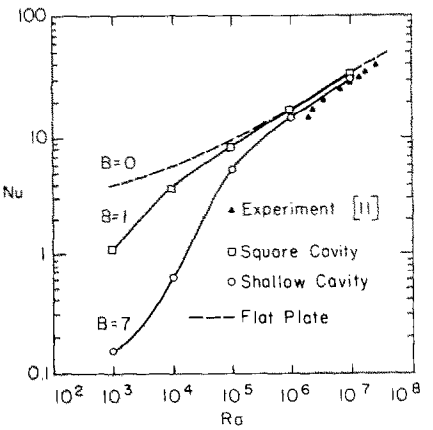

FIG. 13. Variation of Nu with Ra and B.

show that the flow in the shallow cavity remains 'unicellular' throughout. There is no recirculation or secondary cell. The open boundary appears to incur a stabilizing effect by allowing the strongly driven hot fluid to escape freely.

The present numerical study adequately provides the basic flow patterns and heat transfer characteristics for natural convection in a shallow open cavity. It would be interesting to see the effect of including an outer region in the computations. Further studies may also include investigating the effect of variable properties, changing Pr, the aspect ratio and the angle of inclination.

REFERENCES

1. S. Ostrach, Natural convection in enclosures, *Adv. Heat Transfer* **8,** 161–227 (1972).
2. I. Catton, Natural convection in enclosures, Keynote Paper, *Sixth International Heat Transfer Conference*, Toronto, 1978, Vol. 6, pp. 13–43 (1979).
3. F. Penot, Numerical calculation of two-dimensional natural convection in isothermal open cavities, *Numer. Heat Transfer* **5,** 421–437 (1982).
4. O. LeQuere, J. A. C. Humphrey and F. S. Sherman, Numerical calculation of thermally driven two-dimensional unsteady laminar flow in cavities of rectangular cross section, *Numer. Heat Transfer* **4,** 249–283 (1981).
5. J. A. C. Humphrey, L. Miller and K. S. Chen, Experimental investigation of thermally driven flow in open cavities of rectangular cross-section, Mechanical Engineering Report No. FM-81-2, University of California, Berkeley (1981).
6. V. Sernas and I. Kyriakides, Natural convection in an open cavity, *Proceedings of Seventh International Heat Transfer Conference*, München, Germany, Vol. 2, pp. 275–286 (1982).
7. Y. L. Chan and C. L. Tien, A numerical study of two-dimensional natural convection in square open cavities, *Numer. Heat Transfer*, to appear.
8. M. L. Doria, A numerical model for the prediction of two-dimensional unsteady flows of multicomponent gases with strong buoyancy effects and recirculation, Notre Dame Report TR-37191-74-4 (1974).
9. H. R. Jacobs, W. E. Mason and W. T. Hikida, Natural convection in open rectangular cavities, Paper NC 3.2, *Heat Transfer* **3,** 90–94 (1974).
10. H. R. Jacobs and W. E. Mason, Natural convection in open rectangular cavities with adiabatic sidewalls, in *Proceedings of the 1976 Heat Transfer and Fluid Mechanics Institute*. Stanford University Press, pp. 33–46 (1976).
11. Y. L. Chan and C. L. Tien, Laminar natural convection in shallow open cavities, 21st ASME-AIChE National Heat Transfer Conference, *Natural Convection in Enclosures*—1983, HTD. Vol. 26, pp. 77–82 (1983).
12. S. V. Patankar, *Numerical Heat Transfer and Fluid Flow*. McGraw-Hill, New York (1980).
13. Y. L. Chan, Steady laminar natural convection in open rectangular cavities, Ph.D. Dissertation, University of California, Berkeley (1982).
14. D. E. Cormack, L. G. Leal and J. Imberger, Natural convection in a shallow cavity with differentially heated end walls. Part 1: Asymptotic theory, *J. Fluid Mech.* **65,** 209–229 (1974).
15. D. E. Cormack, L. G. Leal and J. H. Seinfield, Natural convection in a shallow cavity with differentially heated end walls. Part 2: Numerical solutions, *J. Fluid Mech.* **65,** 231–246 (1974).
16. J. Imberger, Natural convection in a shallow cavity with differentially heated end walls. Part 3: Experimental results, *J. Fluid Mech.* **65,** 247–260 (1974).
17. W. H. McAdams, *Heat Transmission*, 3rd edn. McGraw-Hill, New York (1954).

UNE ETUDE NUMERIQUE DE CONVECTION NATURELLE LAMINAIRE, BIDIMENSIONNELLE DANS UNE CAVITE OUVERTE ETROITE

Résumé—On étudie numériquement la convection naturelle permanente, laminaire dans une cavité ouverte rectangulaire, bidimensionnelle. Les isothermes et les lignes de courant sont obtenues dans une cavité ouverte et étroite, avec un rapport de forme égal à 0,143, pour des nombres de Rayleigh jusqu'à 10^6, avec des propriétés constantes et les approximations de Boussinesq, en imposant des conditions aux limites à l'ouverture. Cette méthode a été testée et comparée aux cas où les calculs sont conduits dans un domaine externe élargi. Des résultats montrent que les configurations d'écoulement et les résultats de transfert thermique sont gouvernés par des caractéristiques marquées de la cavité chauffée. Ces résultats se comparent bien avec des résultats expérimentaux pour $Ra = 10^6$.

NUMERISCHE UNTERSUCHUNG DER ZWEIDIMENSIONALEN LAMINAREN NATÜRLICHEN KONVEKTION IN FLACHEN, OFFENEN HOHLRÄUMEN

Zusammenfassung—Die laminare stationäre natürliche Konvektion in einem zweidimensionalen, rechteckigen, offenen Hohlraum wird numerisch untersucht. Isothermen und Stromlinien werden in einem flachen, offenen Hohlraum mit einem Seitenverhältnis von 0,143 für Rayleigh-Zahlen bis 10^6 ermittelt, wobei konstante Stoffwerte und die Boussinesq-Näherung verwendet und angenäherte Randbedingungen an der Öffnung angenommen werden. Die Methode wurde getestet und mit anderen verglichen, bei denen die Berechnung in eine ausgedehnte äußere Umgebung fortgesetzt wurde. Die Ergebnisse zeigen, daß die Formen der nach außen führenden Stromlinien und die Wärmeübertragungsvorgänge stark von der Art des beheizten Hohlraums abhängen. Die Ergebnisse stimmen gut mit experimentellen Untersuchungen für $Ra = 10^6$ überein.

ЧИСЛЕННОЕ ИССЛЕДОВАНИЕ ДВУМЕРНОЙ ЛАМИНАРНОЙ ЕСТЕСТВЕННОЙ КОНВЕКЦИИ В ОТКРЫТЫХ ПОЛОСТЯХ МАЛОЙ ВЫСОТЫ

Аннотация—Численно изучена ламинарная стационарная естественная конвекция в двумерных прямоугольных открытых полостях. Используя постоянные свойства и приближение Буссинеска при задании приближенных граничных условий на свободной поверхности полости с отношением сторон 0,143 построены изотермы и линии тока для чисел Рэлея до 10^6. Этот метод был проверен и сравнивался со случаями, в которых расчеты проводились в больших по размеру внешних областях Результаты показывают, что структура вытекающего потока и теплоперенос определяются мощностью нагрева полости. Полученные результаты хорошо согласуются с экспериментальными данными для $Ra = 10^6$.